Journal of the Physical Society of Japan **83**, 064706 (2014)
http://dx.doi.org/10.7566/JPSJ.83.064706

Spin–Orbit Interaction in the Tight-Binding Model —Toward the Comprehension of the Rashba Effect at Surfaces—

Takashi Mii[1,2], Nobuyuki Shima[1,2], Koichi Kano[3], and Kenji Makoshi[1,2*]

[1]*Graduate School of Material Science, University of Hyogo, Kamigori, Hyogo 678-1297, Japan*
[2]*JST-CREST, Kawaguchi, Saitama 332-0012, Japan*
[3]*Graduate School of Department of Physics, Osaka University, Toyonaka, Osaka 560-0043, Japan*

(Received June 20, 2013; accepted February 28, 2014; published online May 15, 2014)

The linear combination of atomic orbitals (LCAO) tight-binding approach is adopted to obtain spin–orbit interaction at surfaces leading to the Rashba effect. Starting from the Dirac equation, the spin–orbit interaction is given by the nonrelativistic limit. All terms, i.e., intra-atomic $\boldsymbol{L}\cdot\boldsymbol{S}$, and spin-flipping transfer matrix elements, are obtained. The tight-binding Hamiltonian is diagonalized resulting in the spin-splitting energy bands for a one-dimensional atomic chain and a two-dimensional triangular atomic sheet. The spin textures induced by the Rashba effect are also revealed.

1. Introduction

It is well known that the nonrelativistic limit of the Dirac equation leads to the spin–orbit interaction in the Hamiltonian,

$$\left\{\frac{p^2}{2m}+V(\boldsymbol{r})+\lambda[\nabla V(\boldsymbol{r})\times\boldsymbol{p}]\cdot\boldsymbol{\sigma}\right\}\psi=E\psi, \tag{1}$$

where λ is the coupling constant given by $\hbar/(4m^2c^2)$. Here, the Zeeman interaction and the Darwin term are omitted. Only when the potential $V(\boldsymbol{r})$ has the spatial spherical symmetry, can the spin–orbit interaction have the form $\boldsymbol{L}\cdot\boldsymbol{S}$. Even if the electronic potential does not have the spatial spherical symmetry, the spatial inversion symmetry of $V(\boldsymbol{r})$ and the time reversal symmetry lead to spin-degenerate electronic states, $\varepsilon(\boldsymbol{k},\sigma)=\varepsilon(\boldsymbol{k},-\sigma)$. In order to use the spin degree of freedom in actual electronic devices, it is necessary to resolve this spin degeneracy.

As Dresselhauss[1] has pointed out the spin–orbit interaction may lead to an unconventional effect, i.e., $\varepsilon(\boldsymbol{k},\sigma)\neq\varepsilon(\boldsymbol{k},-\sigma)$, in a system lacking the spatial inversion symmetry, which comes from the atomic configuration.

Bychokov and Rashba[2] reported that the electronic spin is aligned perpendicular to both the current, $\boldsymbol{p}$, and the electric field, ∇V, in a two-dimensionally confined system or at surfaces, the so-called Rashba effect. In this case, in contrast to the Dresselhaus effect, the spatial inversion symmetry is broken by an (external) electric field. This proposal opened the possibility of controlling electronic spins without the use of a magnetic field or magnetic materials.

Although spin-splitting states are interesting from both theoretical and experimental points of view, the properties of spin-degenerate points should also deserve to be analyzed. Generally spin-degenerate states occur at high-symmetry points in the Brillouin zone like the Γ point, showing Dirac cone structures in energy dispersion and spin texture. Generally, this spin degeneracy is never resolved at a time reversal invariant momentum (TRIM), when a system holds the time reversal symmetry. Being different from the conventional Dirac cone that results, for instance, at the K and K′ points in graphene, the spin-splitting bands form Dirac points in Rashba systems. Recently, the spin-splitting band and Dirac cone structures have been experimentally observed at surface states using spin-resolved photoemission spectroscopy experiments.[3,4]

However, several attempts to explain experimental data on the basis of first-principles theoretical calculations have been successful. Thus, it seems important to analyze the properties of the spin–orbit interaction with a simple model for a qualitative comprehension of physics driven by the spin–orbit interaction.

To clarify the above problem, we studied the band structure and spin texture at surfaces using the linear combination of atomic orbitals (LCAO) tight-binding approach, assuming that the electric field is normal to the surface. Thus, our model can be applied to the study of overlayer structure formed on surfaces or at interfaces. Our approach is rather simple, but effective for developing a fundamental theory and analysing method for (spin-dependent) electronic conductivity on Rashba systems in the future.

2. Model

We adopt the LCAO tight-binding model. At the surface, obviously lacking the inversion symmetry, surface bands split around high-symmetry points in the surface Brillouin zone.

We first give the model potential at surfaces. The predominant effect at a surface is expected to come from the lack of the inversion symmetry normal to the surface. We take the lowest-order term leading to an electric field normal to the surface (z-direction). The potential around each atom is expanded with the spherical harmonics and the leading terms are written as

$$V_n(\boldsymbol{r})=v_n^{\mathrm{s}}+zu_n=v^{\mathrm{s}}(|\boldsymbol{r}-\boldsymbol{R}_n|)+zu(|\boldsymbol{r}-\boldsymbol{R}_n|). \tag{2}$$

Here, $\boldsymbol{R}_n$ is the coordinate of the n site. The second term leads to the Stark effect at each site, which we neglect here.

We add the spin–orbit interaction terms to the Hamiltonian, obtained from the above potential. Defining $\boldsymbol{r}_n=\boldsymbol{r}-\boldsymbol{R}_n$ and $r_n=|\boldsymbol{r}-\boldsymbol{R}_n|$, we obtain

$$\nabla V_n=\frac{\boldsymbol{r}_n}{r_n}\left(\frac{d}{dr_n}v_n^{\mathrm{s}}+z\frac{d}{dr_n}u_n\right)+\hat{z}u_n, \tag{3}$$

where $\hat{z}$ is a unit vector of the z-direction (normal to the surface). We find that the first terms lead to the conventional spin–orbit interaction expressed by $\boldsymbol{L}_n\cdot\boldsymbol{S}$, where $\boldsymbol{L}_n$ is the orbital angular momentum with its center at the nucleus

position of the n site. The last term leads to the spin-flipping transfer between neighboring sites. The spin–orbit interaction of the last part leads to

$$H_{\rm so} = \lambda u_n(|\boldsymbol{r} - \boldsymbol{R}_n|)(\hat{z} \times \boldsymbol{p}) \cdot \boldsymbol{\sigma}, \tag{4}$$

where $\boldsymbol{\sigma}$ is the Pauli spin. The transfer integral obtained from this interaction leads to a spin flip while the electron hops to the neighboring site. For simplicity, we only consider electronic hopping between nearest-neighboring sites.

It is evident that spin-splitting bands do not appear if we take only the local spin–orbit interaction into account, since the spatial inversion symmetry holds in this case. This means that the main ingredient of the Rashba effect is the electron spin flip when an electron is in motion. We notice that this spin-flipping transfer effect affects the energy dispersion and spin textures, i.e., the electronic properties, even for the s-band. Therefore, we make our calculations for the s-orbital for simplicity from now on. For the s-band, the intraatomic spin–orbit interaction vanishes and the calculation becomes extremely simple.

Without the spin–orbit interaction, the transfer matrix element, t, is diagonal for each spin by textbook-like discussion, and is given by

$$t = \langle n + \delta, \sigma | V_n | n, \sigma \rangle, \tag{5}$$

where $n + \delta$ denotes a neighboring site. However, we obtain the spin-flipping transfer with the spin–orbit interaction

$$t_{\sigma\sigma'} = \langle n + \delta, \sigma | u_n(\hat{z} \times \boldsymbol{p}) \cdot \boldsymbol{\sigma} | n, \sigma' \rangle. \tag{6}$$

Note here that the effective magnetic field, $\boldsymbol{B}$, including the g-factor and Bohr magneton, is parallel to the surface and perpendicular to the electron motion:

$$\boldsymbol{B} = u_n(\hat{z} \times \boldsymbol{p}) = u_n(-p_y, p_x, 0). \tag{7}$$

When we define the spin-raising and spin-lowering operators $\sigma_\pm$ by

$$\sigma_\pm = \frac{1}{2}(\sigma_x \pm i\sigma_y), \tag{8}$$

the spin–orbit interaction is rewritten as

$$\begin{aligned} \boldsymbol{B} \cdot \boldsymbol{\sigma} &= (B_x - iB_y)\sigma_+ + (B_x + iB_y)\sigma_- \\ &= B_-\sigma_+ + B_+\sigma_-, \end{aligned} \tag{9}$$

where $B_\pm$ is given by

$$B_\pm = B_x \pm iB_y = \pm iu_n(p_x \pm ip_y). \tag{10}$$

In the next section, we apply this formalism for a one-dimensional (1-D) atomic chain and a two-dimensional (2-D) triangular lattice to see what kind of effect is induced by the spin–orbit interaction, or, in other words, the spin-flipping electronic hopping term.

3. Results and Discussions

Our strategy of diagonalizing the Hamiltonian is as follows.

1) We first form Bloch states consisting of each atomic orbital as

$$|\boldsymbol{k}, \sigma\rangle = \frac{1}{\sqrt{N}} \sum_n e^{i\boldsymbol{k}\cdot\boldsymbol{R}_n} |n, \sigma\rangle. \tag{11}$$

Here, $\boldsymbol{k}$ is a wavevector, n the site number, and N the number of sites involved in the system.

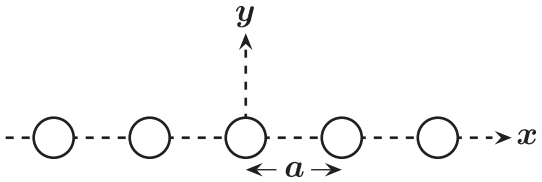

Fig. 1. 1-D atomic array. The substrate surface is in the x–y plane. The inversion symmetry of the potential is broken along the z-direction. The lattice constant is denoted by a.

2) We diagonalize the Hamiltonian at each wavevector $\boldsymbol{k}$. Then, we can obtain the energy bands depending on the structure of the overlayer.

In this study, we demonstrate our results on a 1-D chain and a 2-D triangular lattice. The inclusion of the p-band and the effect of an electric field parallel to the surface will be discussed in separate papers. The former one induces the spin-flipping transition at the same site between different orbitals,[5] and the latter induces the effect of breaking the inversion symmetry not only perpendicular to the surface but also in the in-plane direction.[6]

3.1 One-dimensional chain

We first show our results for 1-D chain states with s-orbitals. Our 1-D atomic array is shown in Fig. 1. Note that each spin state is diagonalized independently, by symmetry, without the spin–orbit interaction:

$$\varepsilon_0(k) = -2t \cos ka, \tag{12}$$

where the center of the band is chosen as the origin of energy, and the transfer matrix element is t. The effect of the crystalline field is neglected. Spin-flipping transfer leads to the term with $\sin ka$ in the off-diagonal elements and the total Hamiltonian is reduced to

$$H_k^{\uparrow\downarrow} = \begin{pmatrix} \varepsilon_0(k) & 2it_{\rm sf} \sin ka \\ -2it_{\rm sf} \sin ka & \varepsilon_0(k) \end{pmatrix}, \tag{13}$$

where the spin-flipping transfer is set to $t_{\rm sf}$ (can be taken as a real quantity). Here, we take the z-axis as a quantization axis of the spin, for simplicity.

Diagonalizing this matrix, we obtain the splitting energy band as

$$\varepsilon_\pm(k) = \varepsilon_0(k) \pm 2|t_{\rm sf} \sin ka|. \tag{14}$$

Here, the subscript $\pm$ indicates upper/lower energy band, respectively. Note that the direction of momentum is parallel to the x-axis in one dimension and the electric field to the z-axis. Then, the effective magnetic field acting on the spin is parallel to the y-axis. If we take the spin quantization axis as the y-axis, our Hamiltonian is diagonal. The dispersion is shifted in k-space because of the complex nature of the transfer matrix elements. The band structure and spin texture are shown in Fig. 2. The parameters are described in the caption.

The results obtained are rather simple, however, we emphasize that the Rashba effect is induced even by s-orbitals, whose angular momentum is zero. The energy bands for the up- and down-spin states are given by phase-shifted cosine functions. Thus, at the TRIM, the origin and edges of the first Brillouin zone, the spin degeneracy is never resolved.

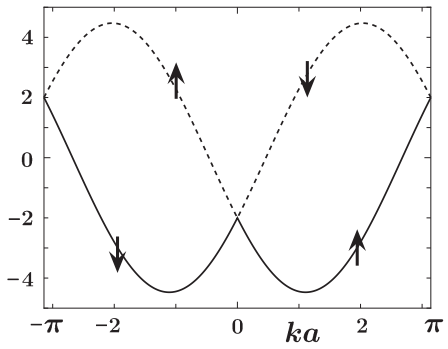

Fig. 2. Energy dispersion of 1-D atomic chain. The energy is scaled by t. The parameter $t_{\rm sf}/t$ is set at 2. The dotted line and solid lines show upper- and lower-energy branches, respectively. One-dimensional Dirac points are seen at the origin and edges of the first Brillouin zone. The up and down arrows in the figure indicate the spin direction for each state with the quantization axis as the y-axis. Namely, for instance, the electronic state of the upper branches with positive and negative momenta have down and up spins, respectively.

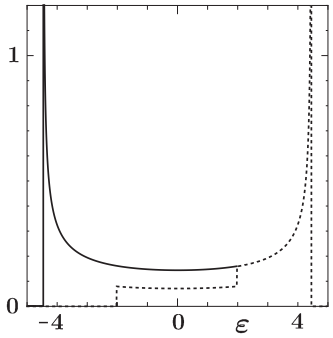

Fig. 3. Density of states for 1-D atomic chain. The parameter, $t_{\rm sf}/t$ is set at 2. The dotted line shows the density of states for the upper-energy branch. Two discontinuity points correspond to two 1-D Dirac points, i.e., the origin and edges of the first Brillouin zone. The solid line together with the dotted line for $\varepsilon > 2$ forms the total density of states, which shows the same function as that in the case without the spin–orbit interaction.

This is because of the time reversal symmetry of the system, i.e., Kramers' degeneracy.

The densities of states are also calculated and shown in Fig. 3. It is clear that the total density of states shows the same function as in the case without the spin–orbit interaction. This is because the spin–orbit interaction gives only positive and negative phase shifts with the same magnitude.

The Dirac point manifests itself in a discontinuity point in the density of states in the case of the 1-D system. For electrons whose energy is located between two Dirac points, two densities of states for the upper and lower branches are energetically overlapped. However, the electronic scattering between the upper and lower bands is prohibited in such a region, since they have opposite spins. This might give rise to a significant effect for electronic transport, which will be reported in another paper. The effect was experimentally observed on the gold surface[7,8] in the two-dimensional case, i.e., the suppression of backscattering because of spin texture.

3.2 Triangular lattice

Here, we show the results for the 2-D triangular lattice shown in Fig. 4, where its first Brillouin zone is also depicted. The energy band without the spin–orbit interaction is obtained as

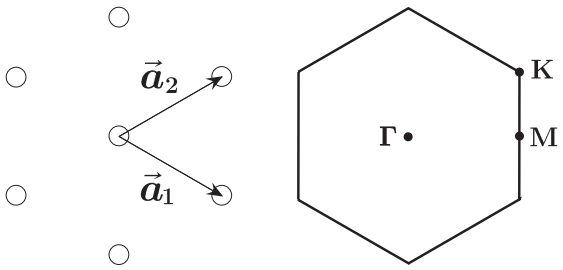

Fig. 4. Triangular atomic array (left side figure) and its first Brillouin zone (right side figure). The primitive lattice vectors $\boldsymbol{a}_1$ and $\boldsymbol{a}_2$, lying on the x–y plane, are drawn. In the first Brillouin zone, the Γ, M, and K points are marked by dots.

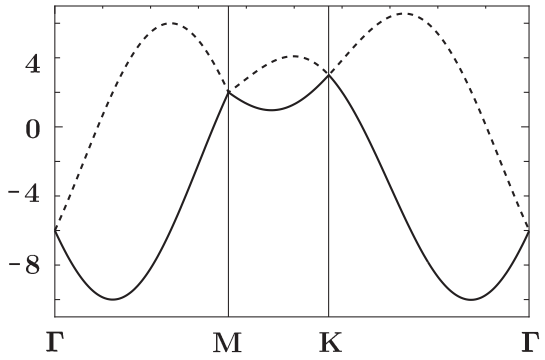

Fig. 5. Energy dispersion for 2-D triangular lattice. The energy is scaled by t, and the parameter $t_{\rm sf}/t$ is set at 2. The dotted and solid lines indicate the upper- and lower-energy branches, respectively. Dirac points emerge not only at Γ and K points, which are the TRIMs, but also the M point, which is not a TRIM.

$$\varepsilon_0(\boldsymbol{k}) = -2t\{\cos \boldsymbol{k}\cdot\boldsymbol{a}_1 + \cos \boldsymbol{k}\cdot\boldsymbol{a}_2 + \cos \boldsymbol{k}\cdot(\boldsymbol{a}_1 - \boldsymbol{a}_2)\}. \quad (15)$$

The spin-flipping effect appears again in the off-diagonal elements:

$$H_{\boldsymbol{k}}^{\uparrow\downarrow} = 2it_{\rm sf}\{e^{i\pi/6}\sin \boldsymbol{k}\cdot\boldsymbol{a}_1 + e^{-i\pi/6}\sin \boldsymbol{k}\cdot\boldsymbol{a}_2 + e^{i\pi/2}\sin \boldsymbol{k}\cdot(\boldsymbol{a}_1 - \boldsymbol{a}_2)\}.$$

By diagonalizing the Hamiltonian, the result is given in the same manner as in the 1-D case:

$$\varepsilon_{\pm}(\boldsymbol{k}) = \varepsilon_0(\boldsymbol{k}) \pm |H_{\boldsymbol{k}}^{\uparrow\downarrow}|. \quad (16)$$

The subscript $\pm$ denotes the upper/lower energy band, respectively. The obtained dispersions are drawn in Fig. 5.

It is reasonable that both branches degenerate at the Γ and M points, which are TRIMs. However, they also degenerate at the K point, which is not a TRIM. This was predicted theoretically on the basis of the group theory[9] and observed experimentally.[3] In this sense, our simple analysis is consistent with those in previous works. Since the off-diagonal elements vanish at the Γ, M, and K points, those degeneracies happen. The energy of each Dirac point does not change even with different spin flip parameter, $t_{\rm sf}$: $\varepsilon_\Gamma = -6t$, $\varepsilon_{\rm M} = 2t$, and $\varepsilon_{\rm K} = 3t$.

The expectation values of spin components are derived analytically,

$$\langle\sigma_x\rangle_{\pm} = \pm\,{\rm Im}[H_{\boldsymbol{k}}^{\uparrow\downarrow}]/|H_{\boldsymbol{k}}^{\uparrow\downarrow}|, \quad (17)$$

$$\langle\sigma_y\rangle_{\pm} = \mp\,{\rm Re}[H_{\boldsymbol{k}}^{\uparrow\downarrow}]/|H_{\boldsymbol{k}}^{\uparrow\downarrow}|, \quad (18)$$

$$\langle\sigma_z\rangle_{\pm} = 0. \quad (19)$$

The spin texture of the upper energy band is shown in Fig. 6.

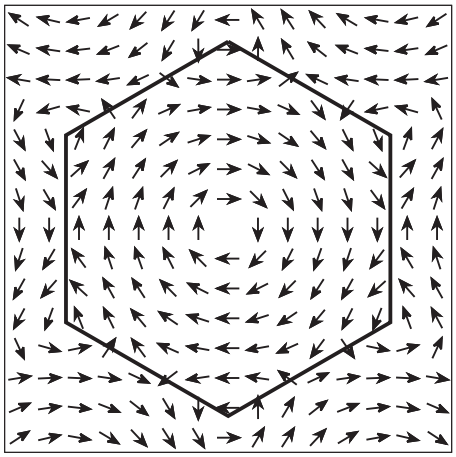

Fig. 6. Spin texture for upper energy branch. The hexagon indicates the first Brillouin zone. It shows a vortical structure at Γ and K points. At the M point, it shows a hyperbolic structure. All of these points are 2-D Dirac points. The spin texture is independent of the parameter t_{sf}/t. The spin texture of lower-energy branch is obtained by reversing all spin directions.

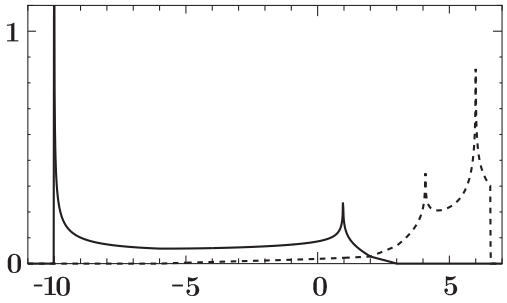

Fig. 7. Density of states for triangular lattice. The dotted and solid lines show upper- and lower-energy branches, respectively. The parameter t/t_{sf} is set at 2. The energy is scaled by t.

The spin texture shows a vortical structure at the Γ and K points, and the hyperbolic structure at the M points. This is also consistent with the experimental results of Bi on Si(111).[3] Although the "hyperbolic" structure also shows vorticity, we use the terminology according to the experimental paper. In Bi/Si(111),[3] the p-orbital might play a crucial role in the Rashba effect. We notice that their results can be reproduced by s-orbitals, and are independent of the Rashba parameter.

The densities of states are calculated and shown in Fig. 7. Being different from those in the case of the 1-D chain, additional van Hove singularities are seen. Other singularities related to Dirac points also come up. In the case of the 2-D system, it shows discontinuity in the first derivative of the density of states. In order to clearly see this singularity, we show a closeup figure of the density of states in Fig. 8. These singularities are seen at the energies at the M and K points, i.e., $\varepsilon_M = 2t$ and $\varepsilon_K = 3t$, respectively. Thus, the same singularity is observed at $\varepsilon_\Gamma = -6t$. The energies of all these Dirac points are independent of the spin flip transfer parameter t_{sf}.

4. Conclusions

In this study, we demonstrated how the spin–orbit interaction leads to the Rashba effect by the LCAO tight-binding approach. The most important factor in such an interaction is the transfer integral. It induces the spin-flip electronic transfer even to the s-orbital, which is the simplest example, as shown in this study. The local $\boldsymbol{L}\cdot\boldsymbol{S}$ term cannot lead to spin-splitting bands, although it modifies the splitting of the p-band owing to the mixture of p-orbitals.

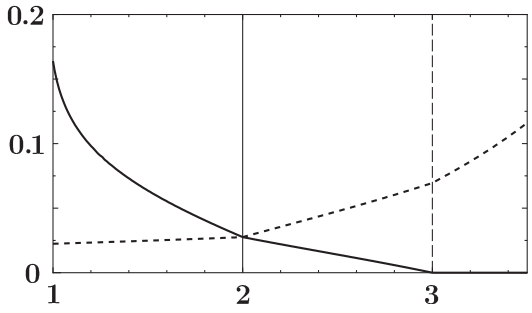

Fig. 8. Density of states for triangular lattice near the M and K points. The dotted and solid lines show upper- and lower-energy branches, respectively. The solid and dashed lines at 2 and 3 indicate the location of energy at the M and K point, respectively.

In the 2-D example, the model we considered here has C_{3v} symmetry including an external electric field. In this case, there is no spin component normal to the surface. Also, the Dirac points emerge at not only the Γ and M points, which are TRIMs, but also the K point, which is not a TRIM.[3] However, in another triangular lattice system, the Tl/Si(111) surface, the spin polarization normal to the surface has been experimentally observed around the K point.[6] The degeneracy at the K point has also been resolved. This effect comes from the lack of mirror symmetry in C_3 and breaking inversion symmetry in the in-plane direction. This effect will be considered in a separate study with an appropriate model potential.[10]

For both 1-D and 2-D models, we have revealed singularities in the density of states, which come from Dirac cone structures. It is clear that the band structure brings the suppression of backscattering because of the spin texture. We are now investigating properties of spin-dependent electronic transport near Dirac points. This study will help us to develop a theory of spin-dependent current in Rashba systems.

*makoshi@sci.u-hyogo.ac.jp

1) G. Dresselhaus, Phys. Rev. **100**, 580 (1955).
2) Y. A. Bychokov and E. I. Rashba, JETP Lett. **39**, 78 (1984).
3) K. Sakamoto, H. Kakuta, K. Sugawara, K. Miyamoto, A. Kimura, T. Kuzumaki, N. Ueno, E. Annese, J. Fujii, A. Kodama, T. Shishidou, H. Namatame, M. Taniguchi, T. Sato, T. Takahashi, and T. Oguchi, Phys. Rev. Lett. **103**, 156801 (2009).
4) K. Yaji, Y. Ohtsubo, S. Hatta, H. Okuyama, K. Miyamoto, T. Okuda, A. Kimura, H. Namatame, M. Taniguchi, and T. Aruga, Nat. Commun. **1**, 17 (2010).
5) L. Petersen and P. Hedegård, Surf. Sci. **459**, 49 (2000).
6) K. Sakamoto, T. Oda, A. Kimura, K. Miyamoto, M. Tsujikawa, A. Imai, N. Ueno, H. Namatame, M. Taniguchi, P. E. J. Eriksson, and R. I. G. Uhrberg, Phys. Rev. Lett. **102**, 096805 (2009).
7) G. Nicolay, F. Reinert, S. Hüfner, and P. Blaha, Phys. Rev. B **65**, 033407 (2001).
8) L. Petersen, P. Laitenberger, E. Lægsgaard, and F. Besenbacher, Phys. Rev. B **58**, 7361 (1998).
9) T. Oguchi and T. Shishidou, J. Phys.: Condens. Matter **21**, 092001 (2009).
10) T. Mii, N. Shima, and K. Makoshi, presented at 29th European Conf. Surface Science (ECOSS29), 2012.